A FRAMEWORK FOR AN ARTIFICIAL NEURAL NETWORK ENABLED SINGLE PIXEL HYPERSPECTRAL IMAGER

Fernando Arias^{1,2}, Heidy Sierra^{1,3} and Emmanuel Arzuaga^{1,2,3}

Laboratory for Applied Remote Sensing, Imaging and Photonics¹
Department of Electrical and Computer Engineering²
Department of Computer Science and Engineering³
University of Puerto Rico Mayaguez, PR, USA.

ABSTRACT

Compressive Sensing enables improvement of acquisition of a variety of signals in various applications with little to no discernible loss in terms of recovered image quality. The current work proposes a signal processing framework for the acquisition and fast reconstruction of compressively sampled hyperspectral images using an artificial neural network architecture. This ANN-based approach is capable of performing a fast reconstruction by avoiding the requirement of solving a computationally intensive image-specific optimization problem. The proposed framework contributes to advance single-pixel hyperspectral imaging device methodologies, which enable a significant reduction in device mechanical complexity, imaging rate, and cost.

Our experiments demonstrate that a hyperspectral image can be reconstructed using only 10% of the samples without compromising classification performance. Specifically, the results show that classification performance of the compressively sampled hyperspectral image recovered using artificial neural networks is equal or higher to that of those obtained using current scanning hyperspectral imaging platforms.

Index Terms— hyperspectral imaging, compressive sensing, deep learning, remote sensing

1. INTRODUCTION

The Compressive Sensing (CS) framework has been used to significantly improve Hyperspectral Image (HSI) acquisition device design, describing improvements in acquisition speed, system complexity and cost [1, 2, 3]. In these approaches, the HSI acquisition system shares a similar design philosophy to the single-pixel camera [4], with the difference that a single measurement operation does not exclusively provide a scalar intensity measurement, but a spectrally resolved linear combination of the target. However, while CS-based approaches provide valuable improvements for acquisition speed and system complexity, they introduce the requirement of finding the computationally expensive solution to an optimization problem. Currently, various algorithms have been proposed for

solving this optimization problem, focused on the specific context of recovering compressively sampled signals [5, 6]. This is a computationally complex and time-consuming operation due to the need of finding optimal, even data-adaptive [7] bases that adequately sparsify specific types of signals, in addition to a variety of method-specific tuning parameters. With optimization-based methods, the process of recovering an image from its compressive measurements can take over 10 minutes for a single frame [8].

In order to mitigate the problem of image recovery times, several ANN-based approaches have been proposed for recovery of images from compressive measurements [9, 10]. These approaches describe similar performance, with small relative differences in recovery quality and execution time behaviors, and show that it is possible to exploit the advantages of both CS and ANNs in conjunction to perform close to real-time CS imaging. While there exists the concern that ANNs require a computationally intensive training process, the reader is reminded that once the training process is complete and its individual weights are determined, ANNs are capable of operating on new data in a negligible amount of time. This property makes ANNs very appealing for computationally complex transformation tasks, such as the case at hand of producing an approximation of spatial signals of interest directly from its compressive samples.

This paper presents a framework for the compressive acquisition and recovery of HSIs. The framework utilizes the CS framework in order to simplify system design and increase HSI acquisition speed, and a trained ANN in order to eliminate the requirement of solving Equation 2 for image recovery. The proposed ANN for image recovery from compressive samples consists of two stages. The first stage, referred to as the Initial Approximation Network (IAN), is based on the ISTA-Net [10] architecture. This stage provides an initial, noisy approximation of the recovered image from compressive samples. The second stage, referred to as the Deep Denoising Network (DDN), removes visual artifacts and further improves image recovery performance. The proposed DDN is based on a residual merge-and-run architecture [11]. Due

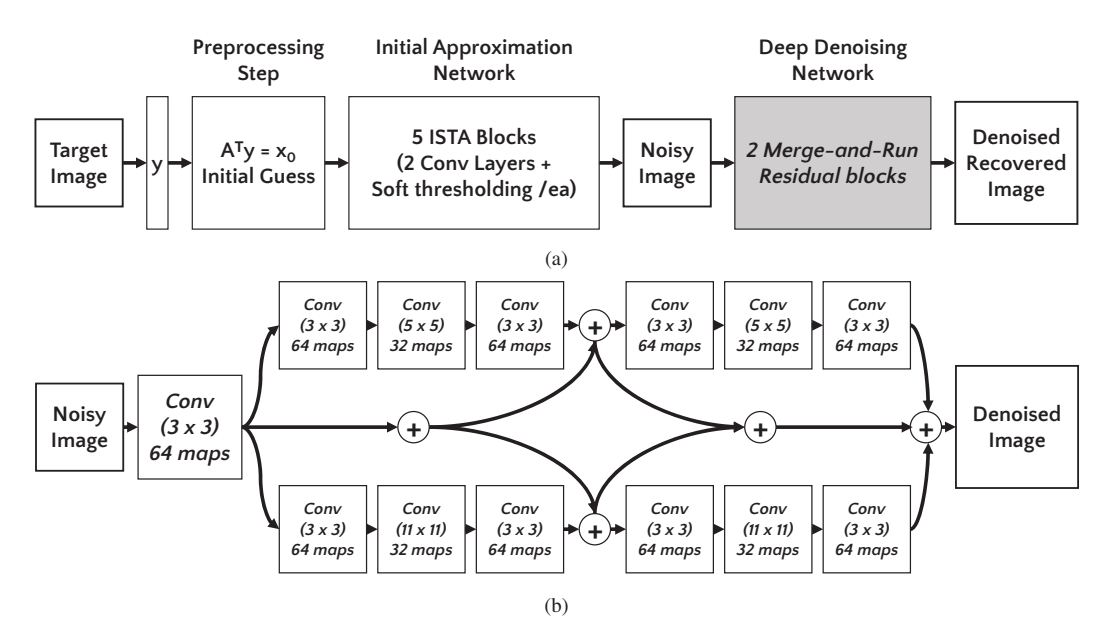


Fig. 1: Proposed framework for fast acquisition and recovery of compressively sampled hyperspectral images. (a) Overall system architecture. (b) Architecture for the proposed Deep Denoiser Network, based on a Merge-and-Run architecture.

to the additive nature of the artifacts introduced by the IAN, we consider this a promising architecture for fine-tuning images. This framework can further enable the development of fully-integrated mobile hyperspectral imaging platforms with reduced constraints on payload size, weight, power and/or on-board computational capabilities.

2. A FRAMEWORK FOR FAST HSI ACQUISITION AND RECOVERY

2.1. Compressive Acquisition of Hyperspectral Images

The CS framework states that a small collection of linear measurements taken from a signal $x \in \mathbb{R}^N$, having a sparse representation in some domain given by a transform operator $\mathbf{T} \in \mathbb{R}^{N \times N}$, contains enough information for its accurate recovery [12, 13]. CS theory states that, if the signal x is sparse, it can be recovered with a high degree of accuracy by taking $M \ll N$ random measurements of x using a known sampling operator matrix $\mathbf{A} \in \mathbb{R}^{M \times N}$. Thus, the array of compressive samples, $y \in \mathbb{R}^M$, is obtained through the operation

$$y = \mathbf{A}\mathbf{T}x. \tag{1}$$

The compressive measurement signal y can be used, in conjunction with the sampling matrix \mathbf{A} to recover an approximation \hat{x} from its compressive measurements by solving the optimization problem:

$$\hat{x} = argmin \|x\|_1 \quad \text{s.t.} \quad y = \mathbf{A}\mathbf{T}x. \tag{2}$$

The proposed framework is based on the foundations provided by previous work on single-pixel hyperspectral cam-

eras. These devices operate in a manner similar to established single-pixel cameras common in CS literature [4], with the important distinction of employing a point spectral measurement device for B wavelengths as a single-pixel sensor [1, 2]. Mathematically, this separates the CS sampling operation presented in Equation 1 into B independent recovery operations, one for each band. This is because each sampling operation that produces a single value of the y vector from linear combinations of the elements of x produces B separate linear combinations using a spectral measurement device. Thus, a high dimensional image $\mathbf{x}_H = \{x_1, x_2, ..., x_B\}$ can be compressively sampled in its full dimensionality into a high dimensional compressive sample vector $\mathbf{y}_H = \{y_1, y_2, ..., y_B\}$ in a simultaneous manner. This process mirrors the acquisition process outlined in Equation 1 for each spectral band. An approximation of the original high dimensional signal $\hat{\mathbf{x}}_H$ can thus be recovered by solving B optimization problems in parallel, as given by Equation 3:

$$\begin{bmatrix} \hat{x_1} \\ \hat{x_2} \\ \dots \\ \hat{x_B} \end{bmatrix} = \begin{bmatrix} \arg\min\|x_1\|_1 & \text{s.t.} & y_1 = \mathbf{A}\mathbf{T}x_1 \\ \arg\min\|x_2\|_1 & \text{s.t.} & y_2 = \mathbf{A}\mathbf{T}x_2 \\ \dots \\ \arg\min\|x_B\|_1 & \text{s.t.} & y_B = \mathbf{A}\mathbf{T}x_B \end{bmatrix}.$$
(3)

2.2. ANN-Based Recovery of Compressively Sampled Images

The problem for recovering HSIs from compressive samples in a bandwise manner presented in Equation 3 is parallelizable, and can be distributed among various computing platforms for increased HSI recovery speed. However, solving

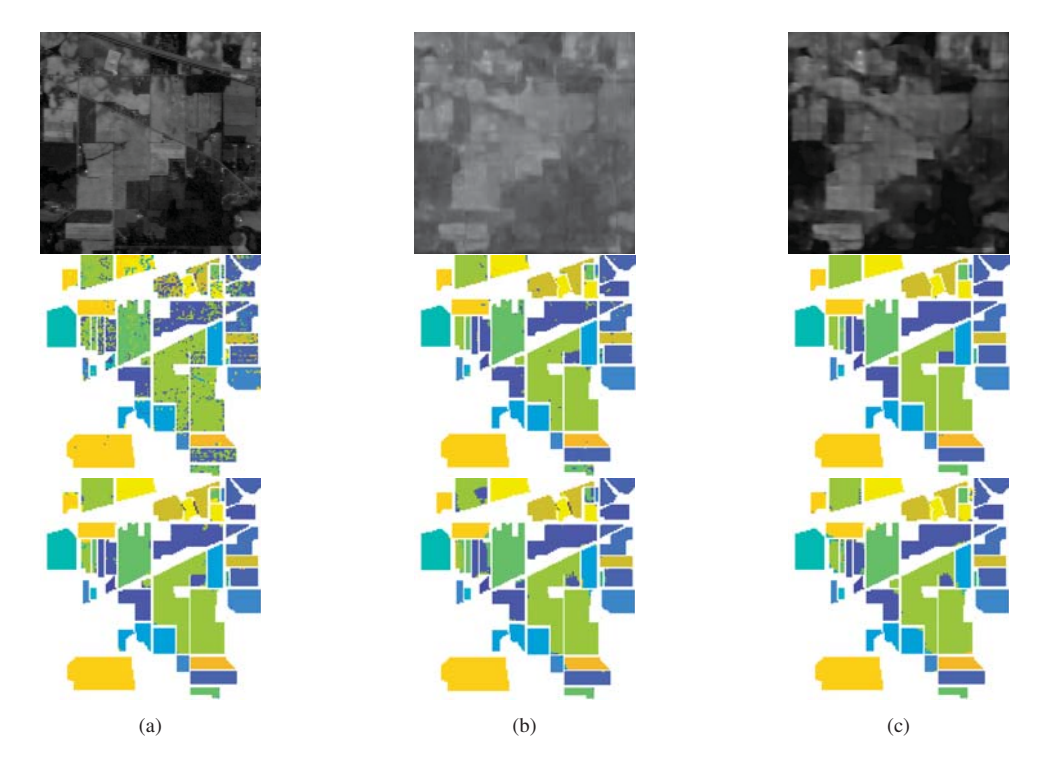


Fig. 2: Images produced at different framework stages with their respective classification maps. Columns from left to right: (a) Reference image, (b) IAN output, (c) DDN output. Rows, from top to bottom: HSI image sample image, cd-LSRC+MD classification maps, CNN-based classifier classification map.

each individual optimization problem is a computationally taxing and time-intensive problem.

In literature, several Artificial Neural Network (ANN) architectures have been proposed for executing fast, nonadaptive image recovery from compressive samples. Most relevant to the current study, are Kulkarni's ReconNet [9], and Zhang's ISTA-Net [10]. Both of these approaches introduce different network architectures for the accurate recovery of CS measurements into their corresponding 2D images. Among these architectures, Zhang's approach consistently more accurate recovery of images (28.50 PSNR vs 26.46 PSNR), at the expense of image recovery rate (25.6 FPS vs 62.5 FPS). Regardless, the fact that the state-of-the-art introduces the possibility to recover individual frames in <1s indicates that it is possible to take advantage of the individual benefits introduced by both CS and ANNs in conjunction to perform approximate real-time CS-based imaging. Due to its scalable, blockwise operation and nonlinear learning qualities, we choose the ISTA-Net architecture, an ANN implementation inspired on the data flow in the ISTA algorithm [6], as the basis for the Initial Approximation Network (IAN) in the current work.

2.3. Hyperspectral Deep Denoiser Architecture

Preliminary work has found that initial recovery of CS images using ISTA-net produces blocking artifacts in recovered images. These can be observed in Figure 2b. In order to compensate for this, we propose the architecture presented in Figure 1, which includes a secondary post-processing network, which is referred to as the Deep Denoising Network (DDN). This post-processing network, presented in Figure 1b, is based on Merge-and-Run architectures [11], which have demonstrated superior abstraction capabilities than traditional Residual Neural Networks (RNN). The purpose of this network, in addition of removing the blocking artifacts introduced by the initial estimation network by performing additive, data-driven corrections to individual block edges, is to further increase the recovery performance of the central region of image blocks recovered from compressive samples.

3. EXPERIMENTAL SETUP

The proposed framework for recovery of HSI data from compressive samples is presented in Figure 1. The training procedure for the recovery framework is performed in two stages. The first stage involves training the IAN, which produces an initial noisy approximation from compressive samples as shown in Figure 1a. The IAN is trained with the

	cdLSRC + MD			CNN		
Class	Original	IAN	DDN	Original	IAN	DDN
1	54.35%	97.83%	100.00%	95.65%	100.00%	100.00%
2	70.31%	95.73%	99.30%	98.60%	93.56%	97.27%
3	64.22%	94.10%	99.52%	97.23%	98.07%	98.92%
4	56.54%	91.98%	100.00%	100.00%	100.00%	100.00%
5	94.41%	97.52%	98.34%	99.79%	96.48%	100.00%
6	98.08%	98.90%	100.00%	95.21%	98.63%	99.73%
7	75.00%	78.57%	85.71%	100.00%	100.00%	100.00%
8	98.74%	99.79%	100.00%	100.00%	99.79%	100.00%
9	40.00%	60.00%	70.00%	100.00%	100.00%	100.00%
10	74.07%	94.24%	99.69%	90.74%	97.22%	98.46%
11	92.10%	98.45%	99.59%	95.97%	92.42%	96.70%
12	58.68%	94.10%	98.15%	97.30%	96.63%	98.99%
13	96.10%	95.61%	99.51%	100.00%	98.05%	100.00%
14	97.23%	98.50%	100.00%	95.02%	99.13%	98.81%
15	59.84%	94.82%	99.48%	100.00%	99.22%	99.22%
16	92.47%	98.92%	100.00%	97.85%	98.92%	97.85%
AA	76.38%	93.07%	96.83%	97.71%	98.01%	99.12%
OA	91.41%	98.19%	99.42%	96.58%	96.21%	98.36%

Table 1: Class-specific classification performance results for two classifiers on the original Indian Pines HSI, the initial approximation from the ISTA-Net Initial Approximation Network (IAN), and the post-processed output from the Deep Denoiser Network (DDN). As additional information, the average class accuracy (AA) and overall pixel accuracy (OA) are presented.

initial guess for the CS samples given by A^Ty as inputs, and the original images as outputs. The architecture used to the current work is based on ISTA-Net and is comprised of five ISTA blocks. Following this, the DDN is trained with the IAN outputs as input data, and the original images as output data. Both the IAN and the DDN were trained on a random selection of $300,000~33\text{px}\times33\text{px}$ blocks extracted from all 220 samples. The networks were trained for 150 epochs using Adam optimization, a learning rate of 0.0001 and a batch size of 128.

Following the image recovery process, the three relevant HSIs (original, IAN output and DDN output) were independently classified using two classifiers: the class-dependent linearized sparse representation classifier with Manhattan Distance information (cdLSRC + MD) [14], and a CNN-based HSI classifier [15].

3.1. Experimental Data

In order to confirm the validity of the proposed method for HSI recovery, we used the $614\text{px} \times 2678\text{px}$ North-South AVIRIS flight line 220-band Hyperspectral image for training the IAN and the DNN networks [16]. For testing recovery and classification performance, we used the 220-band $145\text{px} \times 145\text{px}$, 16-class Indian Pines dataset. For training purposes, the subset corresponding to the Indian Pines HSI was excluded from the selected training samples. The recovered HSIs presented are recovered from compressive measurements with a 10% undersampling rate.

3.2. Results and Discussion

Our analysis produced the classification performance results summarized in Table 1, which presents classification performance on the original Indian Pines HSI, and the recoveries at the IAN and DDN framework stages. These results indicate that both considered HSI classifiers performed better on the DDN network output than the IAN network alone for all classes using the cdLSRC+MD classifier, and most classes using the CNN classifier. Recovered bands from each stage are presented in Figure 2 for illustrative purposes. While a visual inspection of Figure 2 indicates that there exists some degradation of texture information and finer details at 10% undersampling levels, the classification results presented in Table 1 indicate that the information recovered from the acquired compressive samples is sufficient to provide accurate landcover classification of the studied scene.

In addition, Figure 2c confirms the ability of the DDN for improving the quality of the IAN output. Furthermore, the recovered images display higher classification performance in the majority of classes for both classifiers considered. This can be explained due to the spatially contextual low-pass filtering effect introduced by the undersampling operation, and is consistent with results of previous CS applications for HSI classification [17]. We have found that while this process introduces some localized spatial degradation of individual bands, Table 1 indicated that the recovered spectral behavior of pixel regions is sufficient to provide accurate classification results.

4. CONCLUSION

This work presented a signal processing framework based on Compressive Sensing for acquisition, and Artificial Neural Networks for recovery with the objective of improving acquisition and recovery speed of hyperspectral images. In order to evaluate the real-world usability of recovered images, we compared the classification performance of the Indian Pines HSI with its respective approximation from compressive samples. The results obtained indicate that the HSIs recovered using the proposed framework with a 10% sampling rate demonstrate classification performance comparable with HSIs obtained using conventional scanning hyperspectral cameras.

Future work on this subject includes further experimentation with the IAN and DDN architectures to further improve spatial recovery performance of individual bands, as well as work on development of an adaptive scheme that reduces the need for blockwise framework operation. This has the dual benefit of decreasing image handling computation times, and minimizing the introduction of additional noise in recovered images in the form of blocking artifacts.

5. ACKNOWLEDGEMENTS

F.A. is supported by a scholarship grant from the Instituto para la Formacion y Aprovechamiento de Recursos Humanos (IFARHU) office of the government of the Republic of Panama. This work is supported in part by the Laboratory for Applied Remote Sensing, Imaging and Photonics (LARSIP) at the University of Puerto Rico Mayaguez. This material is based upon work supported by the National Science Foundation under Grant No. OAC-1750970.

6. REFERENCES

- [1] Ting Sun and Kevin Kelly, "Compressive sensing hyperspectral imager," in *Computational Optical Sensing and Imaging*. Optical Society of America, 2009, p. CTuA5.
- [2] F Soldevila, E Irles, V Durán, P Clemente, Mercedes Fernández-Alonso, Enrique Tajahuerce, and Jesús Lancis, "Single-pixel polarimetric imaging spectrometer by compressive sensing," *Applied Physics B*, vol. 113, no. 4, pp. 551–558, 2013.
- [3] Gabriel Martín, José M Bioucas-Dias, and Antonio Plaza, "Hyca: A new technique for hyperspectral compressive sensing," *IEEE Transactions on Geoscience and Remote Sensing*, vol. 53, no. 5, pp. 2819–2831, 2015.
- [4] Marco F Duarte, Mark A Davenport, Dharmpal Takhar, Jason N Laska, Ting Sun, Kevin E Kelly, and Richard G Baraniuk, "Single-pixel imaging via compressive sampling," *IEEE Signal Processing Magazine*, vol. 25, no. 2, pp. 83, 2008.
- [5] Maytee Zambrano Nuñez, Fernando X Arias, et al., "Comparative analysis of sparse signal reconstruction. algorithms for compressed sensing.," in *Twelfth LAC-CEI Latin American and Caribbean Conference for Engineering and Technology*, 2014.
- [6] Yudong Zhang, Shuihua Wang, Genlin Ji, and Zhengchao Dong, "Exponential wavelet iterative shrinkage thresholding algorithm with random shift for compressed sensing magnetic resonance imaging," *IEEJ Transactions on Electrical and Electronic Engineering*, vol. 10, no. 1, pp. 116–117, 2015.
- [7] Florian Rousset, Nicolas Ducros, Andrea Farina, Gianluca Valentini, Cosimo D'Andrea, and Françoise Peyrin, "Adaptive basis scan by wavelet prediction for singlepixel imaging," *IEEE Transactions on Computational Imaging*, vol. 3, no. 1, pp. 36–46, 2017.
- [8] Fernando X Arias, Heidy Sierra, Milind Rajadhyaksha, and Emmanuel Arzuaga, "Compressive sensing in reflectance confocal microscopy of skin images: a preliminary comparative study," in *Three-Dimensional and*

- Multidimensional Microscopy: Image Acquisition and Processing XXIII. International Society for Optics and Photonics, 2016, vol. 9713, p. 97130Z.
- [9] Kuldeep Kulkarni, Suhas Lohit, Pavan Turaga, Ronan Kerviche, and Amit Ashok, "Reconnet: Non-iterative reconstruction of images from compressively sensed measurements," in *Proceedings of the IEEE Conference* on Computer Vision and Pattern Recognition, 2016, pp. 449–458.
- [10] Jian Zhang and Bernard Ghanem, "Ista-net: Iterative shrinkage-thresholding algorithm inspired deep network for image compressive sensing," 2017.
- [11] Liming Zhao, Jingdong Wang, Xi Li, Zhuowen Tu, and Wenjun Zeng, "Deep convolutional neural networks with merge-and-run mappings," *arXiv preprint arXiv:1611.07718*, 2016.
- [12] Emmanuel J Candès, Justin Romberg, and Terence Tao, "Robust uncertainty principles: Exact signal reconstruction from highly incomplete frequency information," *Information Theory, IEEE Transactions on*, vol. 52, no. 2, pp. 489–509, 2006.
- [13] David L Donoho, "Compressed sensing," *Information Theory, IEEE Transactions on*, vol. 52, no. 4, pp. 1289–1306, 2006.
- [14] Fernando Arias, Heidy Sierra, and Emmanuel Arzuaga, "Improving execution time for supervised sparse-representation classification of hyperspectral images using the moore-penrose pseudoinverse," *Accepted for Publication the Journal of Applied Remote Sensing*.
- [15] Anirban Santara, Kaustubh Mani, Pranoot Hatwar, Ankit Singh, Ankur Garg, Kirti Padia, and Pabitra Mitra, "Bass net: Band-adaptive spectral-spatial feature learning neural network for hyperspectral image classification," *IEEE Transactions on Geoscience and Remote* Sensing, vol. 55, no. 9, pp. 5293–5301, 2017.
- [16] Marion F. Baumgardner, Larry L. Biehl, and David A. Landgrebe, "220 band aviris hyperspectral image data set: June 12, 1992 indian pine test site 3," Sep 2015.
- [17] Fernando X Arias, Heidy Sierra, and Emmanuel Arzuaga, "Classification performance of a block-compressive sensing algorithm for hyperspectral data processing," in *Algorithms and Technologies for Multispectral, Hyperspectral, and Ultraspectral Imagery XXII.* International Society for Optics and Photonics, 2016, vol. 9840, p. 984005.